

## STRUCTURE-FORMING ROLE OF HEAVY CATIONS IN $\text{Sr}_3\text{B}_2\text{SiO}_8$ ( $\text{Sr}(\text{B},\text{Si})\text{O}_{2.67}$ ) AND $\text{Ba}_3\text{B}_6\text{Si}_2\text{O}_{16}$ BOROSILICATES

S. V. Borisov<sup>1</sup>, N. V. Pervukhina<sup>1,2</sup>,  
and S. A. Magarill<sup>1</sup>

The crystallographic analysis of the orthorhombic (*Pnma*) structure of  $\text{Sr}_3\text{B}_2\text{SiO}_8 \approx (\text{Sr}(\text{B},\text{Si})\text{O}_{2.67})$  shows that its experimentally found symmetry is determined by the geometry of the Sr sublattice where the anion radical without this symmetry simulates it by the statistical averaging of four variants of real configurations. With a reduced fraction of heavy atoms in the triclinic ( $P\bar{1}$ ) structure of  $\text{Ba}_3\text{B}_6\text{Si}_2\text{O}_{16}$ , the Ba and Si cations whose sublattice determines the presence of additional pseudosymmetry form the skeleton of the structure.

**DOI:** 10.1134/S002247661807017X

**Keywords:** crystallographic analysis, cation sublattices, borosilicates, structure stability, pseudosymmetry, crystallographic stoichiometry.

### INTRODUCTION

The problem of combining chemical factors controlling the nearest environment of atoms and crystallographic factors (translational and other symmetries) in the occurrence of crystal structures is very relevant because it is the structure that determines many practically important characteristics of solid materials. One of these characteristics is the structural stability with respect to chemical, mechanical, and thermal actions. Guided by the obvious assumption that the higher the stability is, the fewer degrees of freedom the structure components (atoms, rigid atomic groups of the  $\text{SiO}_4$  type) have - and it is the symmetry that decreases the number of degrees of freedom-we have examined the structure of some prevalent structure types: tourmaline, apatite, garnet, and others [1-3]. When describing the structure of borosilicates, the attention is conventionally drawn to chemically strong coordination polyhedra (with Si-O and B-O bonds), to their distortions and contacts [4-6], while the configuration and resulting symmetry of all components are usually not analyzed. Since it was established that in compositionally similar crystals heavy and large cations played a leading role in the structure organization [1-3], it was of interest to perform the crystallographic analysis of borosilicates with relatively heavy Sr and Ba cations.

### CRYSTALLOGRAPHIC ANALYSIS OF $\text{Sr}_3\text{B}_2\text{SiO}_8$ ( $\text{Sr}(\text{B},\text{Si})\text{O}_{2.67}$ )

The interest in this structure reported in [7] was fueled by some gaps in its description: with the *Pnma* ( $Z=4$ ) symmetry and the unit cell parameters  $a = 12.361 \text{ \AA}$ ,  $b = 3.927 \text{ \AA}$ ,  $c = 5.419 \text{ \AA}$ , ~10.7 oxygen atoms are distributed over 24 positions in a unit cell, out of which 8 are 1/4 occupied and the others are half occupied [7].

---

<sup>1</sup>Nikolaev Institute of Inorganic Chemistry, Siberian Branch, Russian Academy of Sciences, Novosibirsk, Russia; borisov@niic.nsc.ru. <sup>2</sup>Novosibirsk State University, Russia. Translated from *Zhurnal Strukturnoi Khimii*, Vol. 59, No. 7, pp. 1706-1711, September-October, 2018. Original article submitted December 25, 2017.

We used the standard technique to calculate the structural amplitudes for all atoms in the structure ( $F_{\Sigma}$ ), for Sr and (B,Si) cations ( $F_c$ ), only for Sr cations ( $F_{Sr}$ ), for Sr and O atoms ( $F_{Sr+O}$ ), for O atoms ( $F_O$ ). The most intense of them characterizing the crystallographic planes densely occupied by the respective set of atoms are given in Table 1. From the analysis of this table it can be concluded that  $F_c$  intensities slightly differ from  $F_{Sr}$  (for strong  $F_{Sr}$ ), which suggests the absence of substantial joint ordering of Sr and (B,Si) atoms, and for Sr and O there are crystallographic planes densely occupied by these atoms: (600), (020), (312), (420). For Sr atoms, symmetry-related (210), ( $\bar{2}10$ ), and (301) planes should be taken as the coordinate (skeletal) planes of the sublattice. This sublattice will have four Sr-occupied sites in the unit cell volume, and, according to the software from [8], the Sr sublattice will have the parameters  $a_r = 5.47 \text{ \AA}$ ,  $b_r = 5.42 \text{ \AA}$ ,  $c_r = 5.47 \text{ \AA}$ ,  $\alpha_r = 42.01^\circ$ ,  $\beta_r = 47.07^\circ$ ,  $\gamma_r = 42.01^\circ$  (the transition matrix to this subcell is  $\{-1/4 -1/2 3/4 // 0 0 1 // -1/4 1/2 3/4\}$ ). It can be seen that the unit cell of this sublattice is an almost regular acute rhombohedron, for which, and hence for the whole lattice of sites, there is ideally a threefold symmetry axis along the long diagonal equal to the vector sum  $a_r + b_r + c_r = 1/2a - 5/2c$  (i.e., the  $[10\bar{5}]$  direction in the structure). If we pass from this primitive rhombohedron to a lattice with a face-centered rhombohedron [8], then its parameters will be  $a_F = 6.69 \text{ \AA}$ ,  $b_F = 6.75 \text{ \AA}$ ,  $c_F = 6.69 \text{ \AA}$ ,  $\alpha_F = 71.03^\circ$ ,  $\beta_F = 71.86^\circ$ ,  $\gamma_F = 71.03^\circ$  (the transition matrix is  $\{0 -1 -1 // 1/2 0 -1/2 // 0 1 -1\}$ ) that is closer in geometry to a stable cubic  $F$  sublattice. Its long diagonal is also  $1/2a - 5/2c$ .

The ordering of heavy Sr cation positions is the key factor that determines the structure and its symmetry. Thus, the mirror symmetry planes are fixed at the Sr positions forcing the centers of gravity of “rigid” atomic groups  $(\text{B},\text{Si})\text{O}_{4-x}$  and some oxygen atoms of these groups to be fixed on them. However, this fixation requires that one of the edges of the  $(\text{B},\text{Si})\text{O}_4$  tetrahedron should be perpendicular to the mirror symmetry plane, but with its minimum size ( $\sim 2.6 \text{ \AA}$ ) this configuration cannot occur in the system of mirror planes separated by distances  $b/2 \approx 1.96 \text{ \AA}$ . The conflict of chemistry with crystallography is resolved in such a way that this symmetry is absent in each cell, but there are four variants for fixing only the sole  $\text{SiO}_4$  tetrahedron in the unit cell, and this statistics provides an “averaged” mirror symmetry in the structure, thereby increasing its stability [1-3]. On the  $xz$  projection of the structure, Fig. 1a shows its cross-sections by the skeletal planes of the Sr sublattice. Fig. 1b depicts a true structure whose unit cell contains only one  $\text{SiO}_4$  tetrahedron where one of four equivalent positions is fully occupied by oxygen atoms (and, respectively, two positions adjacent on the  $b$  axis will be occupied by the B atoms in triangle coordination). It is quite evident that locally there is also no translational symmetry found experimentally (for example, a multiple increase along the  $b$  axis may be expected). One of possible combinations of the arrangement of the B and Si atoms and the oxygen atoms in general positions is shown in Fig. 1b.

Therefore, the crystal structure of  $\text{Sr}_3\text{B}_2\text{SiO}_8$  ( $\text{Sr}(\text{B},\text{Si})\text{O}_{2.67}$ ) solved at this accuracy level demonstrates the tendency to the maximum symmetry and the minimum unit cell volume, i.e., to the minimum information needed for its description [9]. In this case, it is enough to order the spatial configuration of one component: the heavy Sr cation. The location of other atoms is fitted to this configuration statistically reproducing its higher symmetry.

**TABLE 1.**  $\text{Sr}_3\text{B}_2\text{SiO}_8$  ( $\text{Sr}(\text{B},\text{Si})\text{O}_{2.67}$ ). The Most Atomically Close-Packed Families of Crystallographic Planes: for All Atoms (maximum  $F_{\Sigma}$ ), for Sr and (B,Si) Cations ( $F_c$ ), Only for Sr Cations ( $F_{Sr}$ ), for Sr and O Atoms ( $F_{Sr+O}$ ), for O Atoms ( $F_O$ )

$hkl$	$d_{hkl}$	$F_{\Sigma}$	$F_c$	$F_{Sr}$	$F_{Sr+O}$	$F_O$	$(hkl)_r$	$hkl$	$d_{hkl}$	$F_{\Sigma}$	$F_c$	$F_{Sr}$	$F_{Sr+O}$	$F_O$	$(hkl)_r$
210	3.31	27	112	124	59	85	100, 001	020	1.96	178	120	111	169	58	$\bar{1}01$
301	3.28	112	99	98	112	13	010	312	1.96	154	95	95	154	59	
011	3.17	102	77	71	97	26		511	1.95	114	87	91	118	27	$\bar{1}10$
400	3.09	120	115	109	114	5	101	502	1.83	79	96	99	82	17	
111	3.08	109	89	83	103	20	011	203	1.73	128	93	99	135	35	
102	2.65	30	94	90	26	64		701	1.68	56	91	85	52	33	$\bar{1}\bar{1}\bar{1}$
501	2.25	70	3	11	77	66		420	1.66	141	93	89	137	49	200
112	2.19	88	59	65	94	29		321	1.68	46	80	80	45	34	$\bar{1}11$
600	2.06	128	72	81	138	57		013	1.64	90	108	100	82	18	

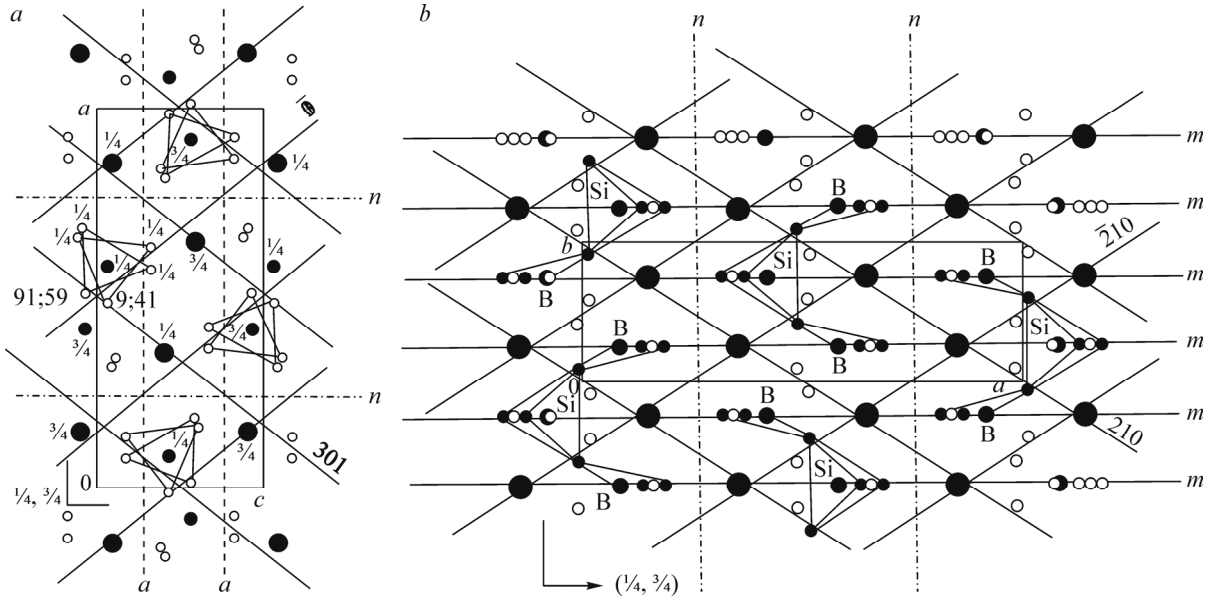


**Fig. 1.**  $\text{Sr}_3\text{B}_2\text{SiO}_8$  ( $\text{Sr}(\text{B},\text{Si})\text{O}_{2.67}$ ): the  $xz$  projection and its cross-sections by the  $(301)$ ,  $(\bar{3}01)$  planes of the Sr sublattice (Sr are large black circles,  $(\text{B},\text{Si})$  are medium black circles, O are small empty circles); the coordinates of four O<sub>2</sub> positions [7] for two  $(\text{B},\text{Si})$  tetrahedra/triangles orientations are indicated in hundredths of the  $b$  axis (a); the  $xy$  projection and its cross-sections by the  $(210)$ ,  $(\bar{2}10)$  planes of the Sr sublattice; one of the possible arrangements of four Sr, one Si, three B, and ten O atoms (small black circles) in a unit cell is shown (b). The projections of  $\text{SiO}_4$  tetrahedra and  $\text{BO}_3$  triangles are shown by thin lines.

With regard to the statistical nature of the oxygen anion distribution, there is no sense in understanding the individual joint Sr+O sublattices in detail. According to [8], one of symmetric sublattices on the  $(020)$ ,  $(600)$ ,  $(312)$  coordinate planes has the parameters  $a' = 2.39 \text{ \AA}$ ,  $b' = 2.47 \text{ \AA}$ ,  $c' = 2.71 \text{ \AA}$ ,  $\alpha' = 56.67^\circ$ ,  $\beta' = 55.40^\circ$ ,  $\gamma' = 71.82^\circ$ . The translation lengths are close to the interatomic Sr–O distances (see [7]), so this sublattice reflects the mutual ordering of large atoms.

## CRYSTALLOGRAPHIC ANALYSIS OF $\text{Ba}_3\text{B}_6\text{Si}_2\text{O}_{16}$

Unlike the previous symmetric structure, this one has a triclinic cell ( $P\bar{1}$ ,  $Z = 1$ ,  $a = 5.038 \text{ \AA}$ ,  $b = 7.6574 \text{ \AA}$ ,  $c = 8.5262 \text{ \AA}$ ,  $\alpha = 77.677^\circ$ ,  $\beta = 77.879^\circ$ ,  $\gamma = 86.324^\circ$  [10]) and a significant excess in the number of light Si and B cations, which can be identified with the centers of “rigid” atomic groups, over heavy Ba cation. Table 2 reports calculated intense  $F_{hkl}$  for different combinations of atoms in the structure. For the most distinct Ba sublattice (i.e., with the maximum ordering of atoms) the  $(012)$ ,  $(\bar{1}\bar{1}1)$ ,  $(1\bar{1}2)$  planes should be taken as the coordinate planes that, according to [8], determine its following parameters:  $a_r = 4.43 \text{ \AA}$ ,  $b_r = 3.57 \text{ \AA}$ ,  $c_r = 3.21 \text{ \AA}$ ,  $\alpha_r = 95.8^\circ$ ,  $\beta_r = 108.8^\circ$ ,  $\gamma_r = 106.9^\circ$ , with the transition matrix to it  $\{-1/7\ 3/7\ 2/7// -4/7\ -2/7\ 1/7// 3/7\ -2/7\ 1/7\}$  with seven sites in the unit cell volume per three Ba atoms. As a rough approximation, this obtuse rhombohedron can be considered primitive for an  $I$ -centered Ba subcell (in a cubic  $I$  cell  $\alpha = \beta = \gamma = 109.5^\circ$ ) and passing to it [8], we obtain a body-centered Ba subcell with  $a_I = 4.55 \text{ \AA}$ ,  $b_I = 4.55 \text{ \AA}$ ,  $c_I = 4.81 \text{ \AA}$ ,  $\alpha_I = 65.0^\circ$ ,  $\beta_I = 83.6^\circ$ ,  $\gamma_I = 90.1^\circ$  with the transition matrix  $\{2/7\ 1/7\ 3/7// -5/7\ 1/7\ 3/7// -1/7\ -4/7\ 2/7\}$ . With a small difference in translation lengths, there is a significant dispersion in angle values indicating an asymmetry in the Ba cation packing. On the other hand, many close-packed planes from Table 2 belong to this subcell:  $(\bar{1}03)$ ,  $(121)$ ,  $(104)$ ,  $(1\bar{2}0)$ ,  $(0\bar{2}3)$ ,  $(201)$ ,  $(\bar{2}11)$ ,  $(\bar{0}31)$ ,  $(041)$ ,  $(230)$ . On the structure projection along the  $a$  axis Fig. 2a shows the cross-sections of the projection by the planes parallel to  $a$ .

For the Ba sublattice with the  $(\text{B},\text{Si})$  cation in the position being 3/4 occupied by silicon,  $(121)$ ,  $(\bar{1}12)$ ,  $(1\bar{1}2)$  were taken as the coordinate planes whose intersections give a subcell with the parameters (according to [8])  $a_c = 3.14 \text{ \AA}$ ,

**TABLE 2.**  $\text{Ba}_3\text{B}_6\text{Si}_2\text{O}_{16}$ . Most atomically close-packed families of crystallographic planes: for all atoms (maximum  $F_{\Sigma}$ ), for cations ( $F_c$ ), for Ba and Si cations ( $F_{\text{Ba+Si}}$ ), for Ba cations ( $F_{\text{Ba}}$ ), for Ba and O atoms ( $F_{\text{Ba+O}}$ ), for O atoms ( $F_O$ )

$hkl$	$d_{hkl}$	$F_{\Sigma}$	$F_c$	$F_{\text{Ba+Si}}$	$F_{\text{Ba}}$	$F_{\text{Ba+O}}$	$F_O$	$(hkl)_K$	$hkl$	$d_{hkl}$	$F_{\Sigma}$	$F_c$	$F_{\text{Ba+Si}}$	$F_{\text{Ba}}$	$F_{\text{Ba+O}}$	$F_O$	$(hkl)_K$
012	3.94	87	126	117	145	106	39		033	2.06	131	134	147	119	115	—	110
021	3.70	125	136	138	125	114	—		004	2.04	96	127	139	114	84	30	011
111	3.34	162	158	165	143	146	—		220	2.04	104	126	135	114	91	23	011
012	3.31	115	130	136	116	108	—		113	2.03	79	—	—	—	85	44	
121	3.13	186	166	184	141	161	—	100	104	2.03	127	91	71	122	158	36	
112	2.97	185	160	174	140	166	26	001	133	2.03	105	89	71	119	134	—	
120	2.95	145	156	168	137	126	—		132	2.02	122	90	67	114	146	32	
112	2.81	181	158	177	126	149	23	010	023	2.01	124	107	95	124	141	—	
113	2.64	118	134	150	117	101	—		024	1.97	113	94	80	113	131	—	
201	2.50	170	160	182	133	143	—		041	1.91	130	109	104	117	138	21	
210	2.35	—	82	69	86	—	46		213	1.89	51	101	92	90	—	49	
031	2.26	144	162	184	129	111	—	101	232	1.83	—	—	—	—	—	43	
103	2.20	114	95	72	12	141	—		123	1.78	116	129	146	104	91	—	111
211	2.17	161	113	94	121	169	48		230	1.77	126	142	159	119	103	—	
211	2.12	104	127	139	110	88	23	110	141	1.74	122	136	151	111	97	—	111
222	2.11	141	111	99	101	131	31		203	1.67	—	125	132	110	104	—	
131	2.08	125	92	77	108	141	33		301	1.68	—	88	84	101	84	—	111
213	2.06	125	115	115	125	135	—	101									

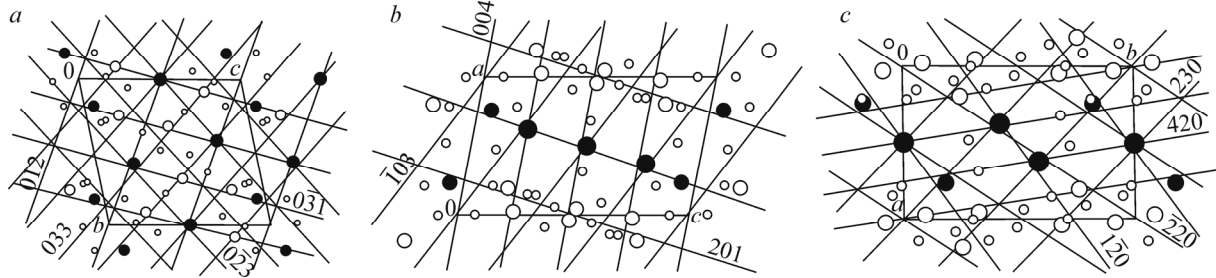


**Fig. 2.**  $\text{Ba}_3\text{B}_6\text{Si}_2\text{O}_{16}$ : the  $yz$  projection and its cross-sections by the  $(012)$ ,  $(0\bar{2}3)$  planes of the Ba sublattice (thick lines) and the  $(033)$ ,  $(0\bar{3}1)$  planes of the  $(\text{Ba+Si})$  sublattice (thin lines) (a); the  $xz$  projection and the  $(201)$ ,  $(\bar{1}03)$  planes of the Ba sublattice,  $(004)$  plane of the  $(\text{Ba+Si})$  sublattice (b); the  $xy$  projection and, respectively, its cross-sections by  $(230)$ ,  $(1\bar{2}0)$  planes of the Ba sublattice and the  $(\bar{2}20)$  plane with the  $(420)$  planes (derivatives of  $(210)$ ) of the  $(\text{Ba+Si})$  sublattice (c). Ba are large black circles, Si are medium black circles, B are medium empty circles, O are small empty circles.

$b_c = 2.81 \text{ \AA}$ ,  $c_c = 2.98 \text{ \AA}$ ,  $\alpha_c = 89.79^\circ$ ,  $\beta_c = 95.26^\circ$ ,  $\gamma_c = 91.68^\circ$  with the transition matrix  $\{1/3 \ 1/3 \ 0// -5/12 \ 1/12 \ 1/4// 1/4 -1/4 \ 1/4\}$  with 12 sites per unit cell. This sublattice is close to a cubic primitive one. A double-volume sublattice with the parameters  $a'_I = 4.10 \text{ \AA}$ ,  $b'_I = 4.13 \text{ \AA}$ ,  $c'_I = 4.15 \text{ \AA}$ ,  $\alpha'_I = 59.13^\circ$ ,  $\beta'_I = 66.47^\circ$ ,  $\gamma'_I = 62.62^\circ$  with the transition matrix  $\{7/12 \ 1/12 \ 3/12// -1/12 \ 5/12 \ 3/12// -2/12 \ -2/12 \ 6/12\}$  will be even more symmetrical. This is an almost regular body-centered rhombohedron which ideally has a threefold symmetry axis along the long diagonal equal to  $1/3\mathbf{a} + 1/3\mathbf{b} + \mathbf{c}$ , i.e., in the [113] crystallographic direction. The  $(0\bar{3}1)$ ,  $(\bar{2}\bar{1}0)$ ,  $(213)$ ,  $(033)$ ,  $(004)$ ,  $(\bar{2}20)$ ,  $(\bar{1}\bar{2}3)$ ,  $(\bar{1}41)$  planes also belong to this sublattice: a substantial part of close-packed planes for both  $(\text{Ba+Si})$  and cation planes containing boron (Table 2). With a certain difference in the parameters of the Ba and  $(\text{Ba+Si})$  sublattices, we can suppose some kind of complex correlation between them, especially because they have some common close-packed planes:  $(121)$ ,  $(1\bar{1}2)$ ,  $(0\bar{3}1)$ .

In conclusion of the analysis, we consider the joint ordering of the heavy and large Ba cation with similar in size, but light oxygen anions. From the analysis of Table 2 it follows that the planes of their close joint packing in a range of  $d_{hkl}$

values comparable with the Ba–O distances will be  $(\bar{2}11)$ ,  $(1\bar{3}1)$ ,  $(104)$ . According to [8], the sublattice on these coordinate planes has the parameters close to those of an acute rhombohedron, from which we can pass to a face-centered, almost orthogonal sublattice with  $a_F = 4.29 \text{ \AA}$ ,  $b_F = 2.96 \text{ \AA}$ ,  $c_F = 4.12 \text{ \AA}$ ,  $\alpha_F = 92.0^\circ$ ,  $\beta_F = 90.2^\circ$ ,  $\gamma_F = 86.93^\circ$ , and the transition matrix  $\{-1/2 -3/8 3/8 // -1/2 1/8 -1/8 // 1/6 -3/8 -7/24\}$ . There are 16 O atoms and three Ba atoms per 24 sites in a unit cell of this sublattice. Fig. 2 depicts all three projections of the structure with their cross-sections by close-packed planes parallel to the axes along which the projections are made. The Ba, Si positions and the position of light B coinciding with the mass center of its “rigid” coordination environment are approximated to the sites of the respective sublattices.

## CONCLUSIONS

The comparison of two structures reveals that in the first one, the number of heavy cations relative to light cations and bulky anions is enough to form a symmetrical framework configuration in which, in addition to the inherent symmetry elements of the *Pnma* group, a “shadow” pseudo axis 3 also exists. In the second structure there are two times more oxygen anions and, respectively, more light Si and B per three heavy cations in a cell. In this context, during the ordering, in addition to the Ba planes, the close-packed planes with the Ba cations and the centers of “rigid” atomic groups (Si and B coordination polyhedra) form. By combined efforts, the inherent symmetry of the structure is brought to  $P\bar{1}$ , but despite a heterogeneous composition, the symmetry of the cation sublattice tends to be higher. Thus, the  $(012)$ ,  $(\bar{1}\bar{1}1)$  and  $(1\bar{1}2)$  planes of the Ba sublattice are related, though very roughly, by pseudo axis 3. The  $(121)$ ,  $(\bar{1}12)$  and  $(1\bar{1}2)$  planes of the (Ba+Sr) sublattice are also related but more strictly. Similar relations are also observed for other close-packed planes of this sublattice (Table 2, last column).

In both structures the true atomic composition does not correspond to the crystallographic stoichiometry. In the first one, to reduce a unit cell volume and increase the symmetry, Si and B are located in a 1/3 and 2/3 ratio in the single position of a light cation [7]. In the second structure the distribution of the B and Si cations over four crystallographic positions is very uneven and only in one of them Si clearly predominates [10].

Inconsistency between the composition and the crystallographic stoichiometry (when each position, i.e., basic atom, is occupied by a certain type of atoms) is a factor that decreases the structure stability. However, the tendency to reduce the diversity (decrease the information capacity of the structure characteristics, namely, the reduction in the number of degrees of freedom of its components) somehow limits this defect, which can be seen from the structures analyzed.

The crystallographic analysis [9] allows us to find out the features of mutual ordering of atomic positions during crystallization, the size and symmetry of pseudotranslational sublattices, and identify the dominant skeleton providing the stability to the structure formed. According to the mechanical-wave concept of the crystal state [9, 11], this skeleton primarily includes the components with a prevailing mass.

## REFERENCES

1. S. V. Borisov, S. A. Magarill, and N. V. Pervukhina. *J. Struct. Chem.*, **2017**, 58(8), 1641-1647.
2. S. V. Borisov, S. A. Magarill, and N. V. Pervukhina. *J. Struct. Chem.*, **2017**, 58(4), 809-812.
3. S. V. Borisov, S. A. Magarill, and N. V. Pervukhina. *J. Struct. Chem.*, **2018**, 59(1), 114-119.
4. L. A. Pautov, A. A. Agakhanov, E. V. Sokolova, and F. C. Hawthorne. *Can. Mineral.*, **2004**, 42, 107-119.
5. F. C. Hawthorne, P. C. Burns, and J. D. Grice. *Rev. Mineral. Geochem.*, **1996**, 33, 41-116.
6. S. K. Filatov and R. S. Bubnova. *Phys. Chem. Glasses*, **2000**, 41, 216-224.
7. M. G. Krzhizhanovskaya, R. S. Bubnova, S. V. Krivivichev, O. L. Belousova, and S. K. Filatov. *J. Solid St. Chem.*, **2010**, 183, 2352-2357.
8. S. A. Gromilov, E. A. Bykova, and S. V. Borisov. *Crystallogr. Rep.*, **2011**, 56(6), 947-952.
9. S. V. Borisov, S. A. Magarill, and N. V. Pervukhina. *J. Struct. Chem.*, **2017**, 58(5), 940-946.
10. M. G. Krzhizhanovskaya, L. A. Gorelova, R. S. Bubnova, and S. K. Filatov. *Z. Kristallogr.*, **2013**, 228, 544-549.
11. S. V. Borisov. *J. Struct. Chem.*, **1992**, 33(6), 871-877.